

RSC Advances

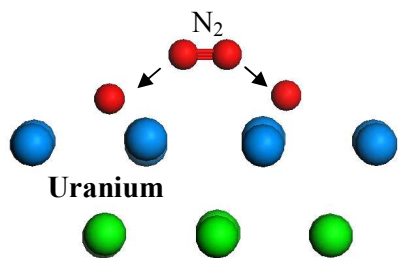


This is an *Accepted Manuscript*, which has been through the Royal Society of Chemistry peer review process and has been accepted for publication.

Accepted Manuscripts are published online shortly after acceptance, before technical editing, formatting and proof reading. Using this free service, authors can make their results available to the community, in citable form, before we publish the edited article. This *Accepted Manuscript* will be replaced by the edited, formatted and paginated article as soon as this is available.

You can find more information about *Accepted Manuscripts* in the [Information for Authors](#).

Please note that technical editing may introduce minor changes to the text and/or graphics, which may alter content. The journal's standard [Terms & Conditions](#) and the [Ethical guidelines](#) still apply. In no event shall the Royal Society of Chemistry be held responsible for any errors or omissions in this *Accepted Manuscript* or any consequences arising from the use of any information it contains.



Nitrogen adsorption and dissociation on α -uranium (001) surface

First-principles study of nitrogen adsorption and dissociation on α -uranium (001) surface

Qiulei Su,[†] Huiqiu Deng,^{†,*} Bingyun Ao,[‡] Shifang Xiao,[†] Piheng Chen,[‡] Wangyu Hu[†]

[†] Department of Applied Physics, School of Physics and Microelectronic Science, Hunan University, Changsha 410082, China

[‡] Science and Technology on Surface Physics and Chemistry Laboratory, P.O. Box 718-35, Mianyang 621907, China

*Corresponding Author

E-mail: hqdeng@hnu.edu.cn; hqdeng@gmail.com

Phone: +86-731-88823226; Fax: +86-731-88822332

ABSTRACT:

The adsorption and dissociation of nitrogen on α -uranium (001) surface have been studied with a first-principles density functional theory (DFT) approach. The effects of strong $5f$ electron-electron correlation and spin-orbit coupling on the adsorption of nitrogen on uranium (001) surface are also discussed. Different coverages of nitrogen atoms and different initial configurations of nitrogen molecules are considered on the uranium surface. The structural parameters and electronic states of nitrogen on uranium surface are obtained. The calculated results indicate that nitrogen atoms are energetically favorable at the hollow sites. The nitrogen molecules adsorbed horizontally on the long-bridge site are found to dissociate completely, and the corresponding adsorption energies are about -4 eV. The electron structure of the most preferred adsorption configuration is investigated, and it is found that the adsorbed nitrogen atoms only seize electrons from the top-most uranium layer. Based on *ab initio* atomistic thermodynamics, the surface phase diagram for nitrogen adsorption on α -uranium (001) surface is obtained and the initial stages of nitridation for uranium surface is discussed.

KEYWORDS: Surface adsorption; Uranium catalyst; Nitridation; Density functional theory; *ab initio* atomistic thermodynamics

1. INTRODUCTION

Uranium (U) is one of the heaviest elements in nature. Until now no other element has such a greatness and evil reputation as that of uranium in the Periodic Table for its applications to nuclear power and potential applications to uranium catalysts.^{1, 2} As early as 1909, it was found that uranium was one of the most efficient catalysts used for the synthesis of ammonia during the Haber-Bosch process.³ In recent decades, numerous reactions were shown to proceed efficiently with participation of uranium-containing catalysts.^{4, 5} In last years the non-aqueous chemistry of uranium has been an active area and there is an increased interest in uranium compounds containing metal–nitrogen multiple bonding.⁶⁻⁹

Dinitrogen is the diatomic molecule with a very strong bond ($945.33 \pm 0.59 \text{ kJ}\cdot\text{mol}^{-1}$), which dominates its chemical properties and makes it difficult to be dissociated. However, small molecules such as nitrogen, carbon monoxide and carbon dioxide can be activated by uranium coordination complexes, which are ascribed to the role of *f* orbitals for binding ligands. Such catalytic advantages of uranium over conventional, transition-metal catalysts have attracted many attentions.¹⁰ In addition, many theoretical efforts have been devoted to studying the activation of nitrogen molecule (N_2). Rochana *et al.*¹¹ investigated the nitrogen adsorption, dissociation, and subsurface diffusion on the V(110) surface, and found a dissociation energy of 0.4 eV. Yeo *et al.*¹² performed first-principles calculations to investigate the full nitridation mechanism for N_2 molecule on and in bcc Fe, and found that the dissociation of N_2 molecule at the strongest adsorption place of hollow site. With *ab initio* techniques and thermodynamics considerations, Soon *et al.*¹³ investigated the interaction between nitrogen atom (N) and Cu(111) surface, and the surface nitride formation was discussed. Zheng *et al.*¹⁴ studied the adsorption of N_2 molecule on the UO(100) surface within DFT framework, and they predicted the lowest energy barrier for dissociation reaction was $266.9 \text{ kJ}\cdot\text{mol}^{-1}$. Wang *et al.*¹⁵ found that the N_2 molecule is moderately activated when

adsorbed on IrO₂(110) surface, which indicated that the IrO₂(110) surface might be applied to catalytic reaction of N₂ fixation.

The electronic structure of uranium is mainly determined by 5*f* electron states which form bands that are very narrow and hybridize with the U 6*d* and 7*s* electronic states. This behavior determines the uranium exotic geometric structure, characterized by atoms bonded in complex and distorted ways.¹⁶ Due to its chemical reactivity, uranium metal will be easily eroded by the oxidation reactions with the O₂, CO or H₂O in atmosphere.¹⁷ Therefore, the protection of uranium surface against air-corrosion is of great challenge in the nuclear engineering field. Surface modification is one of the corrosion-resistant treatments for metallic uranium, and nitridation is a typical surface treatment that can develop good anticorrosion properties by producing thin nitride surface layers on the metal surface. A uranium sesquinitride (α -U₂N₃) layer would be formed on a uranium surface at low substrate temperatures of 230–250 °C during R. F. plasma nitriding process, and it would provide considerable protection against corrosion by other reactive gas, e.g. H₂ and H₂O.¹⁸ Arkush *et al.*¹⁹ used N₂⁺ ion implantation to form thin surface layers with gradual gradients of α -U₂N₃ compounds, which provided a nearly absolute protection against air corrosion. This study is similar to that of Liu *et al.*^{20,21}, who used all-direction ion implantation technology to form a modified nitride layer (α -U₂N₃) on the uranium surface. Corrosion tests indicated that the nitride layer was effective in preventing the matrix from corrosive erosion. Zhang *et al.*²² reported that a nitride layer, mainly composed of UN and U₂N₃, was formed on a uranium surface by excimer laser irradiation, which also showed good anticorrosion properties.

Many researchers have theoretically investigated the interactions between U and some gases in atmosphere, such as O₂, H₂, CO, CO₂ and H₂O.²³⁻²⁹ However, no theoretical work has been done about the interactions between uranium surface and nitrogen. Recently we have carefully discussed the interaction of one single N atom with α -U.³⁰ In that paper, we

systematically studied N adsorption/absorption on U surfaces, N penetration/diffusion in the bulk U, and vacancy trapping for a single N atom in a bulk environment. Continuing that work, in the present paper the adsorption and dissociation behaviors of N₂ molecules onto the α -U(001) surfaces are investigated carefully with first-principles DFT calculation. With *ab initio* atomistic thermodynamics, the N/U(001) surface diagram are also obtained to bridge the energetic information of such stable configurations to the situations of finite temperature and finite pressure, which will shed light on some experimental observations.

2. COMPUTATIONAL DETAILS

All the calculations in the present work were performed using the Vienna *ab initio* simulation package (VASP)^{31,32} based on the DFT framework^{33,34}. The projector augmented wave (PAW) method^{35, 36} was used to describe electron-ion interaction. The electron exchange-correlation was performed within the generalized gradient approximation (GGA) using Perdew–Burke–Ernzerhof (PBE) functional³⁷. Based on the convergence test, the plane-wave cutoff energy was set to 380 eV and the structural relaxations were performed until the residual forces on each atom were less than 0.02 eV/Å. When the relaxed calculations were performed, a broadening approach proposed by Methfessel and Paxton³⁸ was used with $N = 2$ and $\sigma = 0.2$ eV to determine the partial occupancies of each wave function.

The strong correlation effects related to $5f$ electrons have been reported to be important in actinides.³⁹ However, because of uranium's threshold level of f -electron location, the corresponding effects of strong $5f$ electron-electron correlation are weak and many of them can only be observed at low temperature.⁴⁰⁻⁴² Several studies have analyzed the strong correlation problem in uranium recently and found such effects appear to be less crucial. Chantis *et al.*⁴³ used the quasiparticle selfconsistent *GW* method to study the moderate

f-electron correlation effects in α -U and found most of them only appear in the excited-state spectra in the unoccupied *f* states. They concluded that the ground-state properties and the occupied band structure around the Fermi energy were not significantly affected because of the relatively small *f*-electron occupation number in U. Opeil *et al.*^{44, 45} performed photoemission spectroscopy on high quality uranium single crystals and compared the measuring results with first-principles GGA band structure calculations. The favorable agreement between their experimental and theoretical results suggested that strong 5*f* electron-electron correlations effects were not very large in α -U, thus it was reasonable to consider it as a not highly correlated system. Additionally, another challenge for self-consistent electronic structure calculations of heavy elements such as U is the relativistic effect of spin-orbit coupling (SOC). However, previous studies found that this effect was mainly predominant in the unoccupied states and the effect of SOC on the calculated properties was not obvious. Söderlind⁴⁶ studied the elastic and structural properties of uranium metal with DFT-GGA framework, and it was found that the SOC effect on the equilibrium volume, bulk modulus and total energy of α -U was very small. Similar results were also found by Richard *et al.*⁴⁷ during their plane-wave pseudopotential study of the light actinides. They suggested that a more careful treatment of relativistic effects of SOC should be necessary from neptunium on. Taylor⁴⁸ performed first-principles calculations based on PAW formalism to investigate the materials properties of bulk α -U and its (001) surface. Their full spin-orbit and scalar relativistic calculations were shown to give results with similar levels of accuracy compared to experiment.

Nonetheless, we need to validate the strong 5*f* electron-electron correlation effect and the relativistic effect of SOC in the N/U(001) systems, especially on the adsorption energies. Though the standard DFT-GGA mode in its GGA formulation does include exchange and correlation energy, but it has limits to deal with the strong 5*f* electron-electron correlation. The

conventional so-called DFT+ U method⁴⁹ was applied here to deal with the strong correlation effects, in which an additional Hubbard-type term was introduced to address the effective on-site Coulomb interactions among the localized $5f$ orbitals. The rotationally invariant form introduced by Dudarev *et al.*⁵⁰ was used; thus the parameters U and J did not enter separately, and only the difference ($U_{\text{eff}} = U - J$) was meaningful. As Xie *et al.*⁵¹ have systematically investigated the strong correction effects in U metal and finally found a statistical optimal value of 1.24 can improve all the calculated properties. Here we followed their suggestion and took $U_{\text{eff}} = 1.24$ to verify the influence of correlation effects on our research system. In a standard DFT mode with PAW calculations, a fully relativistic effect is restricted to the core-electrons and the valence-electrons are treated with a scalar relativistic approximation^{52, 53}; thus the relativistic effects were considered at least at scalar relativistic level in our N/U(001) system. The GGA+SOC method was applied in some cases to validate the relativistic effect of SOC in the LS -coupling limit.

The structure of uranium crystal depends on temperature at ambient pressure. The crystal structure of bulk α -U, stably existing from 43 K to 940 K, is face-centered orthorhombic (as shown in Figure 1(a)), which belongs to the CmCm space group⁵⁴. Using the $14 \times 7 \times 8$ Monkhorst-Pack⁵⁵ grid for the primitive bulk cell, the shape and volume of the conventional cell were optimized first to verify the strong $5f$ electron-electron correlation and the relativistic SOC effects on the structural properties of bulk α -U. As shown in Table 1, our GGA results compared well with Beeler's⁵⁶ and Taylor's⁴⁸ results. These calculated values also matched well with the experimental results measured at 40 K⁵⁷. When the strong $5f$ electron-electron correlation effects were considered by GGA+ U method, we reproduced Xie's results⁵¹ with $U_{\text{eff}} = 1.24$. It was found that the GGA+ U results were somewhat improved to be closer to the experimental results compared with GGA results. The relativistic effect of SOC was proved to have small impact on the structural parameters of α -U, as also

shown in Table 1. However, as we mainly cared about the N adsorption on α -U(001) surface in present paper, the strong $5f$ electron-electron correlation and the relativistic SOC effects on the adsorption results would be further discussed in the next section.

The adsorption of nitrogen atom and molecule onto the α -U(001) surface was primarily calculated using C(3×2) surface unit cell. The N atom adsorption on a larger C(4×2) surface unit cell was also studied in such a way that more stable N/U(001) adsorption configurations with different coverages would be considered. These two different surface unit cells were both modelled as periodically repeating slabs with five atomic layers (Figure 1(b)), of which the upper two metallic layers were relaxed and the bottom three layers were fixed in their bulk-like positions. A vacuum layer of 12 Å between two successive slabs was thick enough for all the relevant calculations. The nitrogen atom or molecule was placed on one side of the slab where the induced dipole moment was considered by applying a dipole correction⁵⁸. The Brillouin zone was sampled using $4 \times 4 \times 1$ and $3 \times 3 \times 1$ k-meshes for the C(3×2) and C(4×2) surface unit cells, respectively. The computational expense of these simulations was quite substantial that more than two hundred kinds of structures were considered.

The adsorption energies (E_{ads}) of nitrogen on U surfaces are defined in a manner of

$$E_{\text{ads}} = E(\text{U}/\text{N}_m) - E(\text{U}) - \frac{m}{2} E[\text{N}_{2(\text{g})}], \quad (1)$$

where $E(\text{U}/\text{N}_m)$ and $E(\text{U})$ are the total energy of the U slabs with and without nitrogen adsorption, respectively. $E(\text{N}_{2(\text{g})})$ is the energy of an isolated N_2 molecule and it can be obtained by putting one N_2 molecule in a cubic box with 20 Å side-length and carrying out with a Gamma-point calculation. The plane-wave energy cutoff for the N_2 molecule calculation was increased to 600 eV to achieve greater numerical accuracy. The value of m is one or two when a nitrogen atom or molecule is used in the calculation. The calculated bond

length, vibrational frequency and binding energy of N₂ molecule were 1.11 Å, 2422 cm⁻¹ and 10.39 eV, respectively, which agreed well with the reported experimental values⁵⁹ of 1.10 Å, 2359 cm⁻¹ and 9.76 eV.

To study the diffusion kinetics of nitrogen, the Climbing Image Nudged Elastic Band (CI-NEB) Method⁶⁰ was employed to find the minimum energy paths (MEPs) and the transition states. In this method, a chain of linear interpolation images (seven in the present calculations) along an initial pathway between the given initial and final states of a reaction would be relaxed to determine the MEP and its corresponding saddle point. The images were relaxed until the maximum residual forces on each atom are less than 0.02 eV / Å.

3. RESULTS AND DISCUSSION

3.1. Nitrogen Atom Adsorption on α -U(001) Surface and the Effect of Coverage

The adsorption of single N atom on the clean α -U(001) surface was systematically discussed in our previous paper³⁰. As shown in Figure 2, five possible high-symmetry adsorption sites on α -U(001) surface (denoted as top, hollow1, hollow2, long-bridge and short-bridge, respectively) were considered. Previous results proved that only two stable quasi-trigonal sites (hollow1 and hollow2) were preferred for the adsorption of one N atom on α -U (001) surface and the hollow1 site was slightly more energetically stable for N atom adsorption than the hollow2 one. Here we would focus on the strong *5f* electron-electron correlation and the relativistic SOC effects on the N adsorption. Taking C(3 × 2) α -U(001) surface as an example, we calculated the adsorption energies, stable structural parameters and Bader charge⁶¹ with three different approaches, i.e., GGA, GGA+*U* and GGA+SOC. As shown in Table 2, when the strong *5f* electron-electron correlation or relativistic SOC effect was introduced, the largest changes of adsorption energy, N–U bond length and N–surface height were ~4%, ~2% and ~5%, respectively, in comparing with the GGA results.

Furthermore, when compared with the GGA results, the Bader charges of the adsorbed N atom by GGA+*U* or GGA+SOC calculations only changed by 0.01~0.03 |e|. Generally speaking, the adsorptions of nitrogen on α -U (001) surface were not significantly affected by the strong 5*f* electron-electron correlation and the relativistic SOC effects. Thus all the calculations in the following were performed with the standard DFT-GGA calculations, which we think could give reasonable results about the adsorption properties of nitrogen on α -U (001) surface and save a great amount of computation resource.

To understand the properties of the uranium surface adsorbed with more N atoms, we tested the effect of N coverage on the adsorption features. The average adsorption energy (adsorption energy per N atom) is estimated by the following formula

$$E_{\text{average}} = \frac{1}{N_{\text{N}}} [E(\text{U/N}) - E(\text{U}) - \frac{N_{\text{N}}}{2} E(\text{N}_{2(\text{g})})], \quad (2)$$

where $E(\text{U/N})$ is the total energy of the N adsorption configuration, N_{N} denotes the number of adsorbed N atoms. In this section, we took the C(3×2) surface unit cell for example to elaborate the adsorption behaviors of N atoms at various coverages. As listed in Table 3, eight coverages were considered, ranging from 1/12 monolayer (ML) to 1 ML. Moreover, various combinations of N atoms occupying different adsorption sites were studied at certain coverage. Finally, the most stable structure of the corresponding coverage was selected to obtain the average adsorption energy and the corresponding configuration parameters.

We first investigated how the structures change with the number of adsorbed N atoms increasing (as shown in Figure 3). One N adatom preferred to occupy the hollow1 site on α -U(001) surface (Figure 3(a)), as described above. Two N adatoms finally located at two next-nearest neighboring hollow1 sites (Figure 3(b)), producing the most stable structure under the corresponding coverage. Further increasing the coverage to three adsorbed N atoms, the added N atom sequentially resided at another next-nearest neighboring hollow1 site. The

neighboring distance between the adsorbed N atoms were about 3.3 Å, and they finally relaxed to a similar structure of linear nitrine (Figure 3 (c)). It was interesting to see that, for the coverage of 1/3 ML, the four N adatoms eventually formed a periodic zigzag structure on the uranium surface, which consisted of two dinitrogen structures (with the distance of 3.29 Å) and showed the same bond length (about 2.10 Å) to the surrounding U atoms (Figure 3 (d)). As summarized in Table 3, the four low-nitrogen-coverage structures analyzed above demonstrated almost the same $d_{\text{N-surf}}$ and underwent low degree of surface reconstruction. However, the surface U atoms would suffer significant reconstruction as increasing the N coverage, just as the Figures 3(e)-(g) depicted. The U atoms of the topmost layer shifted a lot, especially along the vertical direction, which led to the severe surface wrinkle. When the N coverage was added to 1 ML, all the attached N atoms equally resided the hollow sites, thus the relaxed surface would not reconstruct any more. Rochana *et al.*¹¹ found the reconstruction of V(110) surface when 0.25 ML atomic N was adsorbed at LB site, and more apparent surface reconstruction was observed upon 0.5 ML atomic N adsorption in the β state. Mortensen *et al.*⁶² suggested that at higher N coverage, the islands consisting of C(2 × 2)-N/Fe(100) reconstructed overlayer structures would form on the (111) and (110) surfaces. Kaghazchi *et al.*⁶³ also reported the similar N-induced surface reconstruction that the hcp(1 1 2 1) surfaces of Ru, Os, and Re would break up to form facets of atomically-rough hcp(13 4 2).

To further study the change of the average adsorption energy as a function of nitrogen coverage, we also analyzed the variation of average Bader charge for the corresponding stable structures. As summarized in Table 3, it was found that the average adsorption energy did not change too much at low coverages ($\theta \leq 1/3$ ML), mirroring the trend of the corresponding $d_{\text{N-surf}}$ and average Bader state.

Interestingly, obvious surface reconstruction occurred with the increase of the N coverage

to a critical point of 1/2 ML, and the average Bader charge of the structure unexpectedly arised to a peak value, which can be attributed to the surface wrinkle that provides more bonding U atoms to the absorbed N atoms. Moreover, as the coverage increased to 5/6 ML, the average adsorption energy increased a lot, which agreed well with the decreasing trend of average Bader charge. Additionally, when the surface hollow1 sites were all adsorbed by N atoms, they would be negatively charged because of the strong N–U bonding. The dense charges produced significant lateral coulomb repulsion, which brought about the lowest average absorption energy. Stampfl *et al.* observed similar phenomenon when O atoms were adsorbed on Ru(0001)^{64, 65} and Ag(111)⁶⁵ surfaces. Jiang *et al.*⁶⁶ found lateral repulsions between H atoms on Fe(110) and Fe(100) surfaces, which led to significant destabilization of the adsorbate at higher coverages. Rochana *et al.*¹¹ also reported the lateral interaction between neighboring N atoms on the LB–Top–LB and the TF–TF sites of V(110) surface, which led to weaker adsorption energies than those on the same sites with 0.25ML coverage.

For the ensuing computations, we also investigated the N adsorption behaviors on larger C(4 × 2) surface. With similar analysis methods, a wide range of N coverages were considered to obtain the stable adsorption phases on U surface. Nine varying N coverages of 1/16, 1/8, 1/4, 3/8, 1/2, 5/8, 3/4, 7/8 and 1 ML were selected to find the stable configurations. Finally, the most probable geometries of N atom adsorbed on C(4 × 2) surface unit cell at certain coverages were listed in Figure 4. It was interesting to note that adsorbed N atoms on such surface showed similar structural trend to that of C(3 × 2) surface unit cell with increasing coverages: the hollow1 site was doubtlessly the preferential adsorption site, and periodic zigzag nitrogen configurations occupied U surface with increasing the coverage to 1/4 ML. More intriguingly, two reversed zigzag nitrogen structures existed as the coverage increased to 1/2 ML. On the other hand, large distortion to the surface structure occurred under the coverage ranging from 3/8 ML to 3/4 ML. Additionally, the variation of average

adsorption energies relative to the N coverage was also investigated, just as plotted in Figure 5. We compared such tendency for the two surface unit cells, and found similar results that the average adsorption energies changed little under the coverage of 3/4 ML, but increased a lot with the coverage up to 1 ML. What's more, the energy differences between the two surfaces at the same coverages were also compared. As shown in the inset of Figure 5, the differences at the coverages of 1/4, 1/2, 3/4 and 1 ML were all so modest that we found the largest disparity to be only ~ 0.05 eV, which indicated that geometric factor (the size of the cell) contributed little to the average adsorption characters in such cases.

3.2. Adsorption and Dissociation of Nitrogen Molecule

Dissociative chemisorption is a key step in most surface chemistry, especially for some industrially important catalytic systems. Moreover, prior to the nitriding process of uranium substrate, pure nitrogen gas should be fed to the clean surface. Thus, to study the catalytic properties and nitridation mechanism of uranium surface, the adsorption and dissociation properties of N_2 molecules should be examined in detail. Here one N_2 molecule adsorption on the $C(3 \times 2)$ surface unit cell were studied. As mentioned above, five possible symmetrically distinguishable on-surface sites were taken into account. For each adsorption site, three approaches of the adsorption configurations were obtained based on the orientations of diatomic molecule. Taking the N_2 molecule located at hollow1 site for example, it was denoted as 'Hor1' or 'Hor2' when the molecule was horizontally placed on the α -U(001) surface and its orientation was parallel to x-axis or y-axis of the coordinate system, respectively; and it was denoted as 'Ver' when the molecule was perpendicular to the surface, as illustrated in Figure 6.

N_2 molecule is difficult to be dissociated for its strong triple-bond. Even so, such strong bond strength was weakened when it is adsorbed on α -U(001) surface. The adsorption

energies and optimized adsorption parameters obtained with DFT calculations were listed in Table 4. It was found that there were three kinds of adsorption situations (see Figure 7) for the interactions between N_2 molecule and the U surface. The first one (type-I) was that the N_2 molecule was physically adsorbed on α -U(001) surface, where the N–N bond was slightly lengthened about 0.02 Å than that of free N_2 molecule, and the adsorption energies were $-0.20 \sim -0.60$ eV. The second one (type-II) was that the adsorption energies of the stable configurations range from -1.10 to -2.32 eV, with the N–N bond length of about 1.4 Å, which indicated a dissociative behavior for N_2 molecule. The third one (type-III) was the configuration with the largest adsorption energy, where the N_2 molecule dissociated completely and the two dissociative N atoms were separated remarkably to a distance large than 4.5 Å. In a word, the fate of N_2 molecule depended strongly on the adsorption sites and orientations, which would be elaborated further in the following.

There were two configurations for the physical adsorption of N_2 molecule on α -U(001) surface. After being relaxed, the N_2 molecule initially placed at the short-bridge site with vertical orientation (Ver approach) still kept perpendicular to the surface (denoted as I-1) and the adsorption energy was as low as -0.20 eV, which indicated a weak interaction between the N_2 molecule and U surface. There existed another physical adsorption configuration when the N_2 molecule was initially placed at the top site of U surface with a Ver approach. Although the N_2 molecule tilted to the surface with the angle of 2.25° , it almost stayed at the original top site (denoted as I-2). The N_2 molecule experienced a stronger interaction with the U surface and the adsorption energy was -0.56 eV, which was attributed to the shorter N–U bond length between N atom and its nearest neighboring U atom. The final Hor2 configuration on the top site was nearly degenerate with the final I-2 configuration for that both had similar structural parameters after relaxation.

Several configurations of N_2 molecules on α -U(001) surface involving in chemical

dissociative adsorptions were investigated and they were detailed according to the descending order of E_{ads} in the following. For the relaxed Hor1 configuration at hollow1 site (here denoted as II-1), the adsorption energy was -1.10 eV and two dissociated N atoms finally diffused to the nearby long-bridge sites. The bond length of N–N was elongated to 1.376 Å. The $d_{\text{N-surf}}$ was 1.482 Å, which was significantly shorter than that of physisorption configuration. The N_2 molecule initially placed at short-bridge with Hor1 orientation finally moved to the hollow2 site, with two N atoms dissociated to the nearest long-bridge sites (denoted as II-2). The structural parameters were similar to those of the II-1 configuration analyzed above, but it had a little lower adsorption energy of -1.16 eV. For the N_2 molecules initially located at hollow2 site, both the Ver and Hor2 approaches reached the same final configuration (denoted as II-3) with very similar parameters, and the two dissociative N atoms with larger bond distance of about 1.41 Å stayed close to the surface. The $d_{\text{N-U}}$ was determined to be 2.178 Å, which contributed to the stronger adsorption energy (-1.83 eV). The axis of the diatom was somewhat tilted, with an angle of about 9° relative to the surface level. It was worthwhile pointing out that the four initial configurations, i.e., Ver configurations on hollow1 and long-bridge sites, and Hor2 configurations on hollow1 and short-bridge sites, all relaxed to the semblable structure (denoted as II-4) with almost the same parameters. One dissociative N atom finally occupied the hollow1 site and the other located close to the nearby short-bridge site, and the distance between the neighbor N atoms was 1.406 Å. The adsorption energy, $d_{\text{N-U}}$ and $d_{\text{N-surf}}$ were -2.02 eV, 2.141 Å and 1.438 Å, respectively, which indicated the configuration was more energetically stable than those studied above. For Hor1 approach, the N_2 molecule initially placed at hollow2 or top site shifted to the long-bridge one; then it dissociated and the two dissociative N atoms finally located at the nearest neighboring hollow1 and hollow2 sites (see II-5 structure), which was 1.370 Å away from each other. The average binding height $d_{\text{N-surf}}$ with respect to the surface

was 1.344 Å, which was lower than those of all the structures elaborated above and led to the stronger adsorption energy of -2.32 eV.

Then we focused on two horizontal structures on the long-bridge site, which existed for completely N_2 molecule dissociative adsorption and reached the lowest adsorption energy (approximately -4.0 eV). When the N_2 molecule was placed initially at the long-bridge site with Hor1 approach, two dissociative N atoms were dragged to the hollow1 and hollow2 sites (denoted as III-1), respectively, whose distance was 4.547 Å. The structural parameters d_{N-U} and d_{N-surf} were 2.049 Å and 1.159 Å respectively, which were shorter than those of the five dissociative configurations analyzed above (II-1 to II-5 configurations); this contributed to its lower adsorption energy of -3.93 eV. The N_2 molecule initially located at the long-bridge site with Hor2 orientation finally dissociated to the most stable structure of III-2, where the two N atoms severally diffused to the hollow1 and hollow2 sites. Though the d_{N-U} and d_{N-surf} of III-2 configuration were similar to those of the III-1 one, the larger distance of 4.777 Å between the two N atoms indicated a more complete dissociative adsorption with the lowest adsorption energy of -4.20 eV. However, for H_2 adsorption on α -U (001) surface at the coverages of 0.25 and 0.5 ML, both the horizontal configurations on long-bridge site were found to be unstable.²⁵ As for Fe(100) and Fe(110) surfaces, the N_2 molecules were found to have strong adsorption energies on the hollow sites in both their horizontal and vertical configurations.¹² Furthermore, the N_2 molecule preferred to bind strongly to V(110) surface on the LB and SB sites in a parallel orientation, corresponding to the adsorption energies of -2.82 and -2.27 eV.¹¹

In the previous section, we proved that two isolated N atoms would stably reside the next-nearest neighboring hollow1 sites, producing the most energetically favored configuration under the corresponding coverage. However, the most stable III-2 structure with the N_2 molecule completely dissociated had not relaxed to the above-mentioned state, thus it

was supposed that there exists an energy barrier between these two states, so we calculated the MEP for this reaction. As is shown in Figure 8, the energy profile manifested a very low energy barrier of 0.09 eV, indicating the two dissociative N atoms could easily diffuse to the more stable adjacent hollow sites, even at low temperature. However, Wang *et al.*⁶⁷ studied the dissociation of N₂ molecule on Cu(111) and Au(111), and obtained the energy barriers of more than 3.75 eV. Yeo *et al.*¹² investigated the dissociation of one N₂ molecule, and calculated an energy barrier of 1.15 eV on Fe(100) and 1.18 eV on Fe(110). Rochana *et al.*¹¹ calculated the dissociation path of N₂ molecule on V(110) and found a dissociation barrier of 0.4 eV.

To get the information of the N–U bonding, we performed a detailed study on the electronic structure of the III-2 configuration. By using Bader charge analysis⁶¹, we quantitatively calculated the charge transfer between the dissociative N atoms and the uranium substrate. As listed in Table 5, two N atoms accepted nearly the same net charge of 1.38 |e|, which were almost transferred from their nearby surface U atoms; whereas the U atoms in the 2nd and 3rd layers contributed little to the charge transfer. Therefore, we concluded that there existed obvious ionic bonds between the N atoms and its nearby surface U atoms, which could be attributed to the significant electronegativity difference between N ($K = 3.04$) and U ($K = 1.38$).

Unlike the transition metals, uranium has three *f* electrons, which enable it to catalyze some reactions that are impossible with conventional transition-metal catalysts, especially in the non-aqueous chemistry.¹ To further investigate the orbital contributions to the N–U interaction, we calculated the projected density of states (PDOSs) of an adsorbed N atom and its nearest U atom in the III-2 configuration, and the PDOSs of isolated N atom and the U atom on clean U surface were also calculated for comparison. The contribution of *d* electron to N–U bonding was validated with the *d*-band model⁶⁸, and that of *f*-band was also dealt with the similar way.

As shown in Figure 9, the $2p$ state of isolated N atom was marked at ~ -5 eV by aligning vacuum level with that of clean U(001) surface^{69, 70}, and the Fermi levels for others were aligned to 0 eV. From the PDOS of U atom on clean surface, it was observed that U $5f$ state was dominated at the Fermi level and located from -3 eV to 1.2 eV, while U $6d$ state was relatively broad and located at lower energies (-4.5 eV to 1.2 eV). This was further confirmed by band-center analysis, which revealed the f -band and d -band centers were at -0.2 eV and -2.10 eV, respectively. It was clear from the PDOSs of clean surface U atoms that the $5f$ and $6d$ states at the Fermi level were distinctly reduced due to the N–U bonding, with the d -band and f -band centers shifting from -2.10 eV and -0.20 eV down to -3.17 and -0.60 eV, respectively. It finally exhibited some degree of overlapping and mixing between N $2p$ and U $5f/6d$ orbits within the range of -4.5 eV to -3 eV, which indicated that there also existed some covalent interaction for the N–U bonding. As the d -band center of U atom on clean U surface was closer to the $2p$ states of isolated N atom than that of the f -band center, a stronger mixing between N $2p$ and U $6d$ states was expected than that between N $2p$ and U $5f$ states. This was clearly seen on the PDOSs of adsorbed N atom and the U atom upon adsorption, in which the overlapping between N $2p$ and U $6d$ states, localized in the range -4.5 eV to -3 eV, was much more obvious than that between N $2p$ and U $5f$. This was consistent with general trends developed from d -electron elements, i.e. delocalized sp states (relative delocalized d states in the present case) usually contributed the largest part of the bonding and involved considerable hybridization and charge transfer, while localized d states (more localized f states in the present case) characterize bonding.⁷¹

The ionic part of U–O bonding and the covalent part due to U $5f/6d$ and O $2p$ mixing similarly appeared in the dissociative adsorption of O₂ on α -U (001) surface.^{24, 72} Rochana *et al.*¹¹ described the interaction between N₂ and V(110) with the d -band model, and expected stronger adsorption energy as the d -band shifts up in energy. With GGA approach, Mei *et al.*⁷³

analyzed the bonding behavior in UN, and found similar result that the $2p$ orbitals of N atoms mixed with the $6d$ orbitals of U for some degree below Fermi level. Moreover, Weck *et al.*⁷⁴ investigated the DOS of UN₂, and discovered some degree of $2p-5f$ mixing appears at the top of the valence band, which agreed well with the HSE DOS result reported by Wen *et al.*⁷⁵.

3.3. Surface N/U Phase Diagram with *ab initio* Atomistic Thermodynamics

Even though the most stable N/U(001) configurations under different coverages were studied systematically, the present DFT calculations were merely based on the zero-temperature and non-pressure technique, which introduced a temperature and pressure gap between the theoretical and realistic conditions. In this section, we tried to combine the DFT calculations with the thermodynamic formalism, i.e., *ab initio* atomistic thermodynamics^{64, 76-78}, aiming to obtain the surface phase diagram for equilibrium nitrogen adsorption on α -U(001) surface.

Here we considered the uranium surface to be surrounded by a nitrogen environment, which was described by a nitrogen pressure p and temperature T , and the surface under such realistic conditions would exchange atoms with the chemical reservoirs. Therefore, the surface free energy (γ) of a slab at temperature T and partial pressure p can be calculated as

$$\gamma(T, p, N_U, N_N) = \frac{1}{A} [G(T, p, N_U, N_N) - N_U \mu_U(T, p) - N_N \mu_N(T, p)], \quad (3)$$

where $G(T, p, N_U, N_N)$ is the Gibbs free energy of the system, N_U and N_N are the numbers of U and N atoms in the system, respectively. A is the surface area and μ_U and μ_N are the relevant chemical potentials for uranium and nitrogen atoms, respectively. The Gibbs free energy of the system is given by

$$G(T, p, N_U, N_N) = E(N_U, N_N) + F^{\text{vib}} - TS^{\text{conf}} + pV, \quad (4)$$

where F^{vib} , pV and TS^{conf} terms can be safely neglected for typical pressure and temperature⁷⁸.

⁷⁹, and $E(N_U, N_N)$ is the total energy of the system calculated by first-principles approach.

Thus, we get a simplified form of the Gibbs free energy of adsorption with respect to the clean surface, which can be expressed as

$$\begin{aligned}\Delta G(T, p) &= \gamma(T, p, N_U, N_N) - \gamma_{\text{clean}}(T, p, N_U, 0) \\ &= \frac{1}{A} [E(N_U, N_N) - E(N_U, 0) - N_N \mu_N].\end{aligned}\quad (5)$$

To calculate the values of the chemical potential for nitrogen atom, we use

$$\mu_N = \frac{1}{2} E_{N_2} + \Delta \mu_N(T, p), \quad (6)$$

where

$$\Delta \mu_N(T, p) = \mu(T, p^0) + \frac{1}{2} k_B T \ln\left(\frac{p}{p^0}\right). \quad (7)$$

Here p^0 corresponds to standard atmospheric pressure and $\mu(T, p^0)$ can be obtained from thermochemical tables⁸⁰. By incorporating Equations (2) and (6) into Equation (5), we can get

$$\Delta G(T, p) = \frac{N_N}{A} [E_{\text{average}} - \Delta \mu_N(T, p)], \quad (8)$$

which determines the most stable structure under specified temperature and partial pressure of nitrogen.

As is shown in Figure 10, the energetically preferred structures at every considered coverages were depicted in the phase diagram; and three typical temperatures (300, 600 and 900 K) were selected to correlate the nitrogen chemical potential with the pressure. A natural starting point to analyze the surface phase diagram was the leftmost part, which represented the vanishing concentrations of N/U(001) surface phase species and indicated that clean α -U(001) surface would be the most stable system state under the corresponding $\Delta \mu_N$ of -2.20 eV. For a slightly higher $\Delta \mu_N$, ranging from -2.20 eV to -2.14 eV, the structure of C(3 \times 2)-1/3 ML emerged to be more stable, and the C(4 \times 2)-6/16 ML configuration exhibited a

higher ΔG when $\Delta\mu_{\text{N}}$ was increased to a higher range of -2.14 eV to -2.10 eV, resulting to a more favorable phase. Despite of the same number of the adsorbed N atoms, the $\text{C}(3 \times 2)_{-1/2}$ ML configuration showed a steeper slope with higher coverage, which made it become more stable for $\Delta\mu_{\text{N}} > -2.10$ eV. By further increasing the nitrogen concentration, i.e., moving the red vertical line to a larger value of -1.83 eV in the surface phase diagram, the structure of $\text{C}(3 \times 2)_{-3/4}$ ML would gradually become more populated, which occupied a large domain in the phase diagram. Apart from these on-surface phases discussed above, we also investigated an ensuing state with 1 ML nitrogen atoms adsorbed on the surface and another 1 ML atoms diffused into the sub-surface interstitial sites. What's more, by further increase the $\Delta\mu_{\text{N}}$ to a larger value of -1.17 eV, we would intriguingly find a direct phase transition to $\text{C}(4 \times 2)_{-2}$ ML state without undergoing the corresponding $\text{C}(4 \times 2)_{-1}$ ML surface structure, which indicated that the 1 ML on-surface configuration never corresponds to a thermodynamically stable phase.

4. CONCLUSION

In the present work, we systematically investigated the adsorption of nitrogen atoms and the dissociation of nitrogen molecules on $\alpha\text{-U}(001)$ surface, as well as the surface phase diagram for the adsorption of nitrogen on the $\alpha\text{-U}(001)$ surface through DFT calculations. The strong $5f$ electron-electron correlation and the relativistic SOC effects on the adsorption of nitrogen on the $\text{C}(3 \times 2)$ $\alpha\text{-U}(001)$ surface were tested and it was found that the adsorption energies, structural parameters and Bader charge were not significantly affected.

The effect of N-coverage (ranging from $1/12\text{ML}$ to 1ML) on the adsorption features were investigated. For low coverage ($\theta \leq 1/3$ ML), the nitrogen adatoms continuously located the next-nearest neighboring hollow sites, and composed a periodic zigzag chain at the coverage of $1/3$ ML. The surface U atoms reconstructed severely at higher coverage, and such

phenomenon disappeared until the N atoms fully covered the surface, with each adsorbate equally residing the hollow sites and leading to the weakest average absorption energy, which was attributed to the significant lateral coulomb repulsion among the adatoms.

The dissociative adsorption of N_2 molecule was also investigated with three different orientations at five adsorption sites. It was found that two horizontal structures on the long-bridge site existed for completely N_2 dissociative adsorption with the adsorption energies of about 4 eV, and it was easy to overcome the low energy barrier of 0.09 eV to reach the most stable configuration where two N atoms stably resided the next-nearest neighboring hollow sites. Two dissociative N atoms accepted the same net charge of 1.38 |e| from their nearby surface U atoms, and the electronic structures exhibited some degree of overlapping and mixing between N $2p$ and U $5f/6d$ states within the range of -4.5 eV to -3 eV.

Finally, the surface phase diagram for equilibrium nitrogen adsorption on α -U(001) surface was obtained by *ab initio* atomistic thermodynamics. It was found that clean U(001) surface would be the most stable system state under the corresponding $\Delta\mu_N$ of -2.20 eV, and with increasing the value of $\Delta\mu_N$, several structures of $C(3 \times 2)$ - $1/3$ ML, $C(4 \times 2)$ - $3/8$ ML, $C(3 \times 2)$ - $1/2$ ML and $C(3 \times 2)$ - $3/4$ ML gradually became the favorable phase. It was interesting to find a direct phase transition from $C(3 \times 2)$ - $3/4$ ML to $C(4 \times 2)$ - 2 ML state when the $\Delta\mu_N$ was larger than -1.17 eV.

ACKNOWLEDGEMENT

We gratefully acknowledge many helpful discussions with Dr. Zhenhua Zeng (Purdue University). This work was financially supported by the National Natural Science Foundation of China (NSFC-NSAF 10976009, NSFC 51371080). The work was carried out at National Supercomputer Centers in Changsha and Tianjin, and the calculations were performed on TianHe-1(A).

REFERENCES

1. A. R. Fox, S. C. Bart, K. Meyer and C. C. Cummins, *Nature*, 2008, **455**, 341-349.
2. M. J. Monreal and P. L. Diaconescu, *Nature chemistry*, 2010, **2**, 424-424.
3. F. Haber, *German patent DE*, 1909, **229126**.
4. T. Andrea and M. S. Eisen, *Chemical Society Reviews*, 2008, **37**, 550-567.
5. Z. Ismagilov and S. Lazareva, *Catalysis Reviews*, 2013, **55**, 135-209.
6. C. M. Camp, J. Pécaut and M. Mazzanti, *Journal of the American Chemical Society*, 2013, **135**, 12101-12111.
7. A. P. Sattelberger and M. J. Johnson, *Science*, 2012, **337**, 652-653.
8. D. M. King, F. Tuna, E. J. L. McInnes, J. McMaster, W. Lewis, A. J. Blake and S. T. Liddle, *Science*, 2012, **337**, 717-720.
9. R. K. Thomson, T. Cantat, B. L. Scott, D. E. Morris, E. R. Batista and J. L. Kiplinger, *Nature chemistry*, 2010, **2**, 723-729.
10. I. Castro-Rodríguez and K. Meyer, *Chemical communications*, 2006, 1353-1368.
11. P. Rochana, K. Lee and J. Wilcox, *The Journal of Physical Chemistry C*, 2014, **118**, 4238-4249.
12. S. C. Yeo, S. S. Han and H. M. Lee, *Physical Chemistry Chemical Physics*, 2013, **15**, 5186-5192.
13. A. Soon, L. Wong, M. Lee, M. Todorova, B. Delley and C. Stampfl, *Surface Science*, 2007, **601**, 4775-4785.
14. J. Zheng, C. Lu, B. Sun and W. Chen, *Acta Physico-Chimica Sinica*, 2008, **24**, 1995-1999.
15. C. C. Wang, S. S. Siao and J. C. Jiang, *The Journal of Physical Chemistry C*, 2010, **114**, 18588-18593.
16. P. Söderlind, O. Eriksson, B. Johansson, J. M. Wills and A. M. Boring, *Nature*, 1995, **374**, 524-525.

17. G. X. Li, S. Wu, Nuclear Fuel; S. Wu Eds.; Chemical Industry Press: Beijing, 2007.
18. A. Raveh, R. Arkush, S. Zalkind and M. Brill, *Surface and Coatings Technology*, 1996, **82**, 38-41.
19. R. Arkush, M. Mintz and N. Shamir, *Journal of nuclear materials*, 2000, **281**, 182-190.
20. Z. Long, K. Liu, B. Bai and D. Yan, *Journal of Alloys and Compounds*, 2010, **491**, 252-257.
21. K. Liu, R. Bin, H. Xiao, Z. Long, Z. Hong, H. Yang and S. Wu, *Applied Surface Science*, 2013, **265**, 389-392.
22. Y. Zhang, D. Meng, Q. Xu and Y. Zhang, *Journal of nuclear materials*, 2010, **397**, 31-35.
23. M. B. Shuai, H. R. Hai, X. Wang, P. J. Zhao and A. M. Tian, *Journal of Molecular Structure: THEOCHEM*, 2001, **536**, 269-276.
24. G. Li, W. H. Luo and H. C. Chen, *Chemical Research and Application*, 2010, **10**, 012.
25. J. L. Nie, H. Y. Xiao, X. T. Zu and F. Gao, *Journal of Physics: Condensed Matter*, 2008, **20**, 445001.
26. S. Senanayake, A. Soon, A. Kohlmeyer, T. Söhnle and H. Idriss, *Journal of Vacuum Science & Technology A: Vacuum, Surfaces, and Films*, 2005, **23**, 1078.
27. G. Li, W. H. Luo and H. C. Chen, *Acta Physico-Chimica Sinica*, 2010, **26**, 1378-1384.
28. G. Li, W. H. Luo and H. C. Chen, *Acta Physico-Chimica Sinica*, 2011, **27**, 2319-2325.
29. B. Xiong, D. Meng, W. Xue, Z. Zhu, G. Jiang and H. Wang, *Acta Physico Sinica*, 2003, **57**, 1617-1623.
30. Q. L. Su, H. Q. Deng, B. Y. Ao, S. F. Xiao, X. F. Li, P. H. Chen and W. Y. Hu, *Journal of Applied Physics*, 2014, **115**, 164902.
31. G. Kresse and J. Hafner, *Physical Review B*, 1993, **47**, 558.
32. G. Kresse and J. Furthmüller, *Physical Review B*, 1996, **54**, 11169.
33. P. Hohenberg and W. Kohn, *Physical review*, 1964, **136**, B864.
34. W. Kohn and L. J. Sham, *Physical Review*, 1965, **140**, A1133.

35. G. Kresse and D. Joubert, *Physical Review B*, 1999, **59**, 1758.
36. P. E. Blöchl, *Physical Review B*, 1994, **50**, 17953.
37. J. P. Perdew, K. Burke and M. Ernzerhof, *Physical review letters*, 1996, **77**, 3865-3868.
38. M. Methfessel and A. Paxton, *Physical Review B*, 1989, **40**, 3616.
39. A. J. Freeman, G. Lander and C. Keller, *Handbook on the Physics and Chemistry of the Actinides*, North-Holland Amsterdam, 1984.
40. G. Lander, E. Fisher and S. Bader, *Advances in physics*, 1994, **43**, 1-111.
41. L. Fast, O. Eriksson, B. Johansson, J. Wills, G. Straub, H. Roeder and L. Nordström, *Physical review letters*, 1998, **81**, 2978.
42. A. Lawson, B. Artinez, J. Roberts, B. Bennett and J. Richardson Jr, *Philosophical Magazine B*, 2000, **80**, 53-59.
43. A. N. Chantis, R. Albers, M. Jones, M. van Schilfgaarde and T. Kotani, *Physical Review B*, 2008, **78**, 081101.
44. C. Opeil, R. Schulze, M. Manley, J. Lashley, W. Hults, R. Hanrahan Jr, J. Smith, B. Mihaila, K. Blagoev and R. Albers, *Physical Review B*, 2006, **73**, 165109.
45. C. Opeil, R. Schulze, H. Volz, J. Lashley, M. Manley, W. Hults, R. Hanrahan Jr, J. Smith, B. Mihaila and K. Blagoev, *Physical Review B*, 2007, **75**, 045120.
46. P. Söderlind, *Physical Review B*, 2002, **66**, 085113.
47. N. Richard, S. Bernard, F. Jollet and M. Torrent, *Physical Review B*, 2002, **66**, 235112.
48. C. D. Taylor, *Physical Review B*, 2008, **77**, 094119.
49. V. I. Anisimov, F. Aryasetiawan and A. Lichtenstein, *Journal of Physics: Condensed Matter*, 1997, **9**, 767.

50. S. Dudarev, G. Botton, S. Savrasov, C. Humphreys and A. Sutton, *Physical Review B*, 1998, **57**, 1505-1509.
51. W. Xie, W. Xiong, C. A. Marianetti and D. Morgan, *Physical Review B*, 2013, **88**, 235128.
52. L. Kleinman, *Physical Review B*, 1980, **21**, 2630.
53. A. MacDonald, W. Pickett and D. Koelling, *Journal of Physics C: Solid State Physics*, 1980, **13**, 2675.
54. D. A. Young, *Phase diagrams of the elements*, University of California Pr, 1991.
55. H. J. Monkhorst and J. D. Pack, *Physical Review B*, 1976, **13**, 5188-5192.
56. B. Beeler, C. Deo, M. Baskes and M. Okuniewski, *Journal of Nuclear Materials*, 2013, **433**, 143-151.
57. C. S. Barrett, M. H. Mueller and R. L. Hitterman, *Physical Review*, 1963, **129**, 625-629.
58. J. Neugebauer and M. Scheffler, *Physical Review B*, 1992, **46**, 16067.
59. W. M. Haynes, D. R. Lide and T. J. Bruno, *CRC Handbook of Chemistry and Physics 2012-2013*, CRC press, 2012.
60. G. Henkelman, B. P. Uberuaga and H. Jónsson, *The Journal of Chemical Physics*, 2000, **113**, 9901.
61. R. F. Bader, *Atoms in molecules*, Wiley Online Library, 1990.
62. J. J. Mortensen, M. Ganduglia-Pirovano, L. B. Hansen, B. Hammer, P. Stoltze and J. K. Nørskov, *Surface Science*, 1999, **422**, 8-16.
63. P. Kaghazchi and T. Jacob, *Physical Chemistry Chemical Physics*, 2012, **14**, 13903-13906.
64. C. Stampfl and M. Scheffler, *Physical Review B*, 1996, **54**, 2868.
65. C. Stampfl, *Catalysis today*, 2005, **105**, 17-35.
66. D. Jiang and E. A. Carter, *Physical Review B*, 2004, **70**, 064102.
67. G. C. Wang, L. Jiang, X. Y. Pang and J. Nakamura, *The Journal of Physical Chemistry B*, 2005, **109**, 17943-17950.

68. B. Hammer and J. K. Nørskov, *Advances in catalysis*, 2000, **45**, 71-129.
69. M. E. Björketun, Z. Zeng, R. Ahmed, V. Tripkovic, K. S. Thygesen and J. Rossmeisl, *Chemical Physics Letters*, 2013, **555**, 145-148.
70. Z. H. Zeng, H. Q. Deng, W. X. Li and W. Y. Hu, *Acta Physica Sinica*, 2006, **55**, 3157.
71. F. Abild-Pedersen, J. Greeley, F. Studt, J. Rossmeisl, T. Munter, P. G. Moses, E. Skulason, T. Bligaard and J. K. Nørskov, *Physical review letters*, 2007, **99**, 016105.
72. J. L. Nie, L. Ao, X. T. Zu and H. Gao, *Journal of Physics and Chemistry of Solids*, 2014, **75**, 130-135.
73. Z. G. Mei, M. Stan and B. Pichler, *Journal of Nuclear Materials*, 2013, **440**, 63-69.
74. P. F. Weck, E. Kim, N. Balakrishnan, F. Poineau, C. B. Yeaman and K. R. Czerwinski, *Chemical physics letters*, 2007, **443**, 82-86.
75. X. D. Wen, R. L. Martin, G. E. Scuseria, S. P. Rudin and E. R. Batista, *The Journal of Physical Chemistry C*, 2013, **117**, 13122-13128.
76. X. G. Wang, A. Chaka and M. Scheffler, *Physical review letters*, 2000, **84**, 3650.
77. C. Stampfl, H. Kreuzer, S. Payne, H. Pfnür and M. Scheffler, *Physical review letters*, 1999, **83**, 2993.
78. K. Reuter and M. Scheffler, *Physical Review B*, 2001, **65**, 035406.
79. J. R. Kitchin, K. Reuter and M. Scheffler, *Physical Review B*, 2008, **77**, 075437.
80. M. W. Chase, J. Curnutt, H. Prophet, R. McDonald and A. Syverud, *Journal of physical and chemical reference data*, 1975, **4**, 1-176.

Table 1. Structural parameters for ground state α -U. Results calculated with different *ab initio* approaches and the experimental observation at 40 K are listed in the table. *a*, *b* and *c* are the lattice constants and *y* is the internal parameter; *V* represents the volume per atom.

Approach		<i>a</i> (Å)	<i>b/a</i>	<i>c/a</i>	<i>y</i>	<i>V</i> (Å ³)
GGA	PBE(This work)	2.796	2.091	1.752	0.098	20.04
	PBE(Beeler ⁵⁶)	2.793	2.094	1.752	0.098	19.99
	PW91(Taylor ⁴⁸)	2.800	2.106	1.748	0.097	20.19
GGA+ <i>U</i> (1.24)	PBE(This work)	2.849	2.060	1.742	0.100	20.74
	PBE(Xie ⁵¹)	2.840	2.074	1.747	0.100	20.75
GGA+SOC	PBE(This work)	2.795	2.094	1.755	0.099	20.06
	PW91(Taylor ⁴⁸)	2.797	2.098	1.749	0.098	20.07
Experiment ⁵⁷		2.836	2.068	1.740	0.102	20.52

Table 2. Energetic, structural parameters and Bader charge for N atom adsorbed on α -U(001) C(3×2) surface. E_{ads} denotes the adsorption energy according to Eq. (1); $d_{\text{N-U}}$ represents the shortest binding length between N and U atoms; $d_{\text{N-surf}}$ is the average binding height from N atom to the first layer; Bader charge represents the average charge states of absorbed N atom.

Approach	stable N site	E_{ads} (eV)	$d_{\text{N-U}}$ (Å)	$d_{\text{N-surf}}$ (Å)	Bader Charge (e)
GGA	hollow1	-2.09	2.176	1.110	1.42
	hollow2	-2.03	2.092	1.149	1.39
GGA+ <i>U</i>	hollow1	-2.18	2.175	1.069	1.43
	hollow2	-2.10	2.108	1.091	1.41
GGA+SOC	hollow1	-2.17	2.141	1.069	1.44
	hollow2	-2.12	2.085	1.093	1.42

Table 3. The average adsorption energies and structural parameters for various coverages of N atoms on α -U(001) C(3×2) surface. ΔZ represents the degree of surface wrinkle, which indicates the maximum perpendicular distance between two surface U atoms.

C(3×2)	Coverage (ML)							
	1/12	1/6	1/4	1/3	1/2	3/4	5/6	1
E_{ads} (eV)	-2.09	-2.17	-2.18	-2.20	-2.17	-2.05	-1.89	-1.24
$d_{\text{N-surf}}$ (Å)	1.110	1.101	1.093	1.093	–	–	–	1.133
ΔZ (Å)	0.153	0.305	0.240	0.479	1.438	1.264	2.397	0
Bader charge (e)	1.42	1.38	1.37	1.37	1.46	1.42	1.37	1.17

Table 4. Adsorption energies and geometric parameters of the N₂ molecule adsorbed on α -U(001) surface calculated for different sites and approaches. d_{N-N} represents the nitrogen-to-nitrogen distance upon adsorption; d_{N-U} represents the shortest binding length between N and U atoms; β represents the angle between the N–N bond and the surface level; FS represents the final structure.

approach	initial N ₂ site	E_{ads} (eV)	d_{N-N} (Å)	d_{N-U} (Å)	$d_{N-\text{surf}}$ (Å)	β (°)	FS
Ver	hollow1	-2.02	1.406	2.139	1.438	11.03	II-4
	hollow2	-1.83	1.409	2.177	1.438	8.93	II-3
	longbride	-2.02	1.406	2.141	1.438	10.96	II-4
	short-bridge	-0.20	1.149	2.607	2.779	85.24	I-1
	top	-0.56	1.143	2.411	2.975	87.75	I-2
Hor1	hollow1	-1.10	1.376	2.206	1.482	0	II-1
	hollow2	-2.32	1.370	2.297	1.344	0	II-5
	longbride	-3.93	4.547	2.049	1.159	0	III-1
	short-bridge	-1.16	1.384	2.222	1.413	0	II-2
	top	-2.32	1.371	2.295	1.344	0	II-5
Hor2	hollow1	-2.02	1.406	2.141	1.438	11.11	II-4
	hollow2	-1.83	1.410	2.178	1.438	9.01	II-3
	longbride	-4.20	4.777	2.066	1.161	0.97	III-2
	short-bridge	-2.02	1.407	2.141	1.438	11.08	II-4
	top	-0.56	1.143	2.410	2.975	87.54	I-2

Table 5. Bader charges of two dissociative nitrogen adatoms and the uranium atoms in the three surface layers. A negative charge value indicates gaining electrons, whereas a positive value indicates losing electrons.

Net charge of each atom												
2 N	1.38					1.38						
1 st _U	-0.45	-0.32	-0.54	-0.39	-0.49	-0.41	-0.03	-0.01	-0.01	-0.03	-0.11	-0.04
2 nd _U	0	-0.01	0	0.02	0.02	0.02	0	0.01	0	0	0.01	0
3 rd _U	0	0	0	0	0	0	0	0	0	0	0	0

FIGURE CAPTIONS:

Figure 1. Schematic views of the (a) bulk α -U and (b) slab model for α -U(001) surface.

Figure 2. Schematic illustrations of the α -U(001) surface cells and adsorption sites, where H1 = hollow1 site, H2 = hollow2 site, LB = long bridge site, SB = short bridge site, and T = top site. Blue and green spheres denote the first and second layer of uranium slab, respectively.

Figure 3. Top and side views of the most stable configurations for different nitrogen coverages on α -U(001) C(3 × 2) surface: (a) 1 N (1/12 ML); (b) 2 N (1/6 ML); (c) 3 N (1/4 ML); (d) 4 N (1/3 ML); (e) 6 N (1/2 ML); (f) 9 N (3/4 ML); (g) 10 N (5/6 ML); (h) 12 N (1 ML).

Figure 4. Top and side views of the most stable configurations for different nitrogen coverages on the C(4 × 2) surface: (a) 1 N (1/16 ML); (b) 2 N (1/8 ML); (c) 4 N (1/4 ML); (d) 6 N (3/8 ML); (e) 8 N (1/2 ML); (f) 10 N (5/8 ML); (g) 12 N (3/4 ML); (h) 14 N (7/8 ML); (i) 16 N (1 ML).

Figure 5. Average adsorption energy vs. nitrogen coverage of C(3 × 2) and C(4 × 2) surface unit cells. Inset: the average adsorption energy differences between C(4 × 2) and C(3 × 2) surfaces at four same coverages.

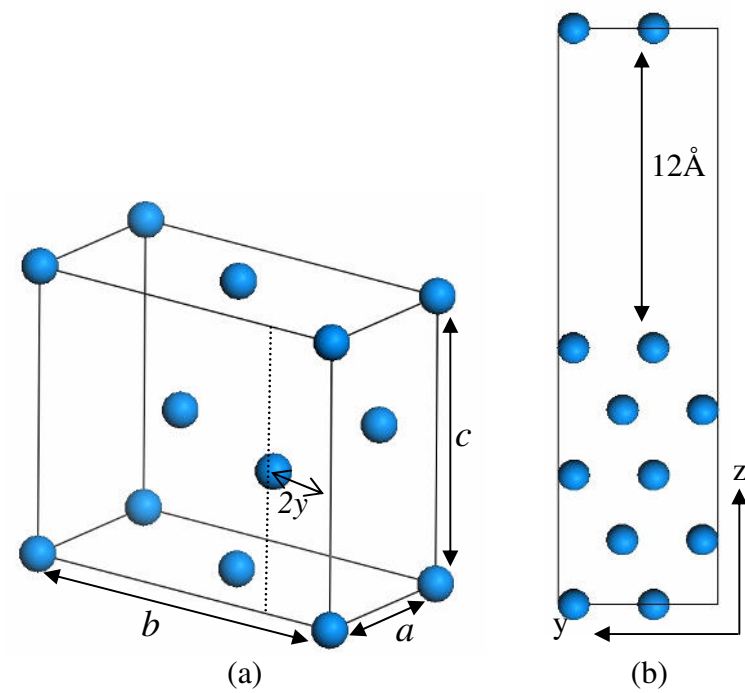
Figure 6. Horizontal and vertical adsorption configuration for N₂ on the Hollow1 site: (a) top view of the Hor1 configuration, (b) top view of the Hor2 configuration, (c) top view of the Ver configuration, (d) side view of the Ver configuration.

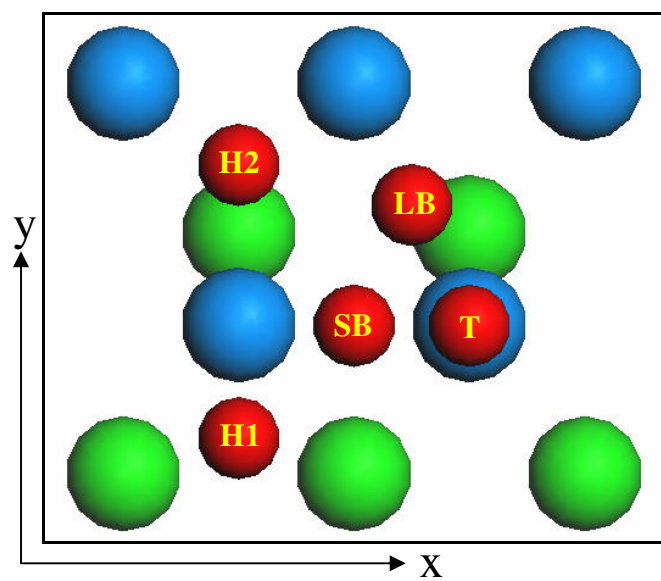
Figure 7. Top and side views of the the optimized structures of N₂ adsorption onto α -U(001) surface.

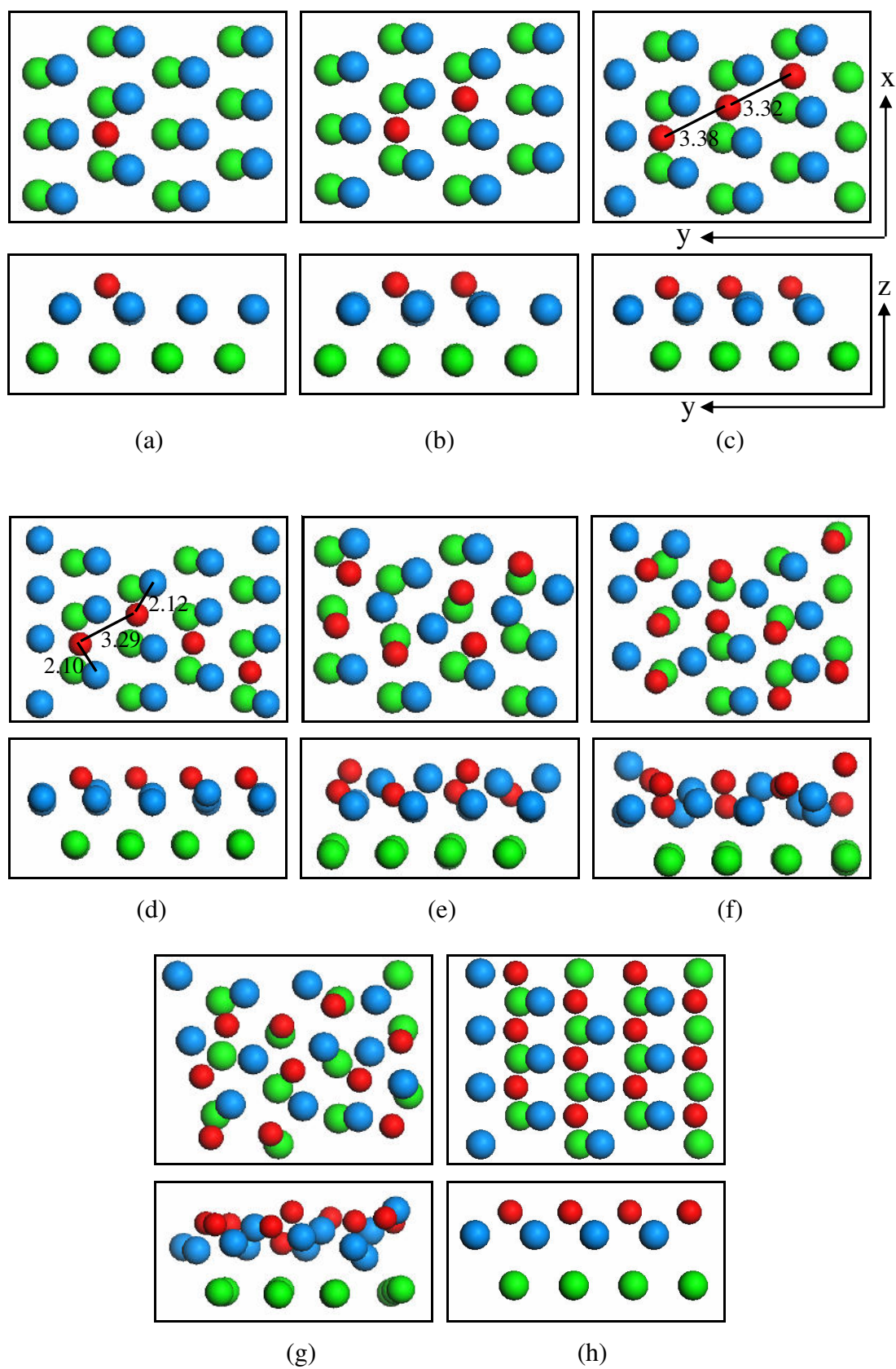
Figure 8. The MEP between the most completely N₂ dissociative adsorption structure and the more stable structure with two nitrogen atoms adsorbed.

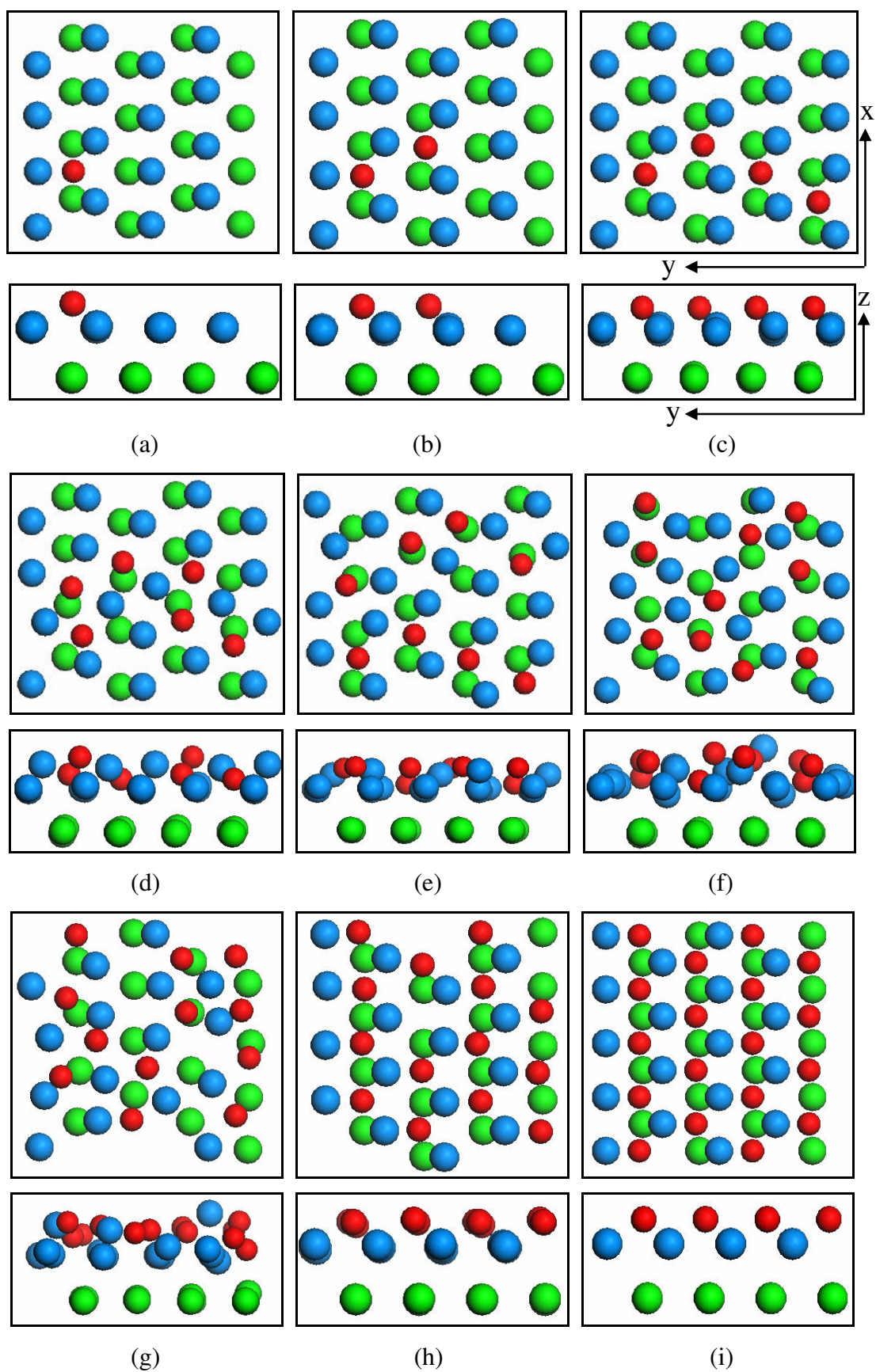
Figure 9. PDOS of an adsorbed N atom and its nearest U atom. PDOS of the corresponding U atom on the bare surface is superimposed for comparison, and the green arrow denotes the 2*p* state of isolated N atom by aligning vacuum level with that of bare U surface. (dash lines: before adsorption, solid lines: after adsorption).

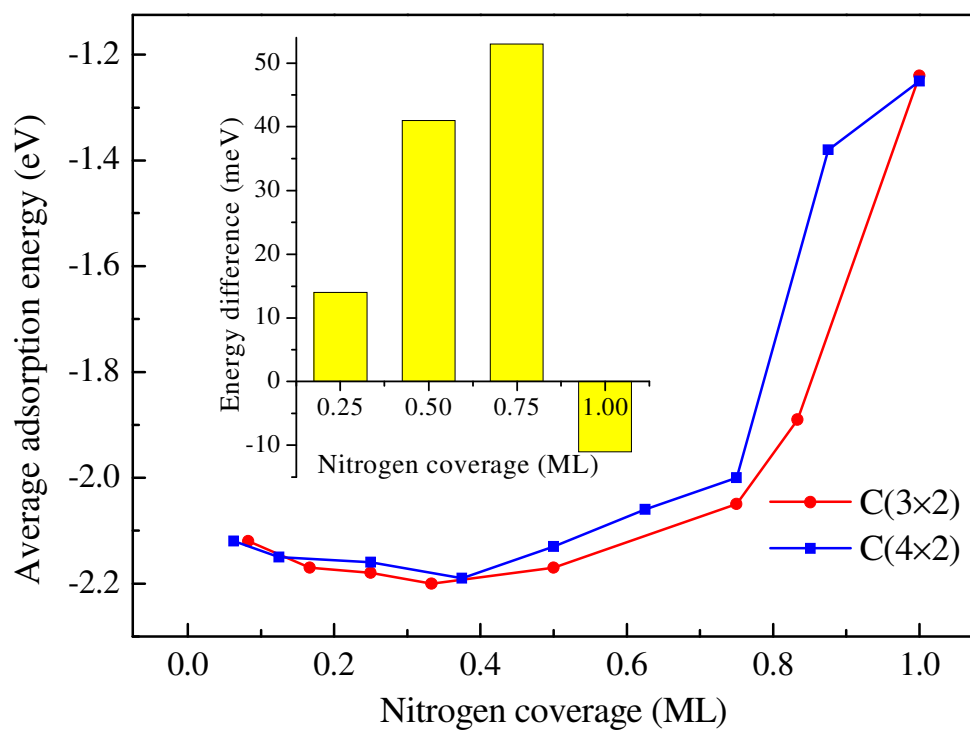
Figure 10. The calculated Gibbs energy of adsorption energy ΔG for surface structures versus the nitrogen chemical potential $\Delta\mu_{\text{N}}$: all unfavorable adsorption phases are indicated in grey, while colored think lines indicate thermodynamically stable phases.

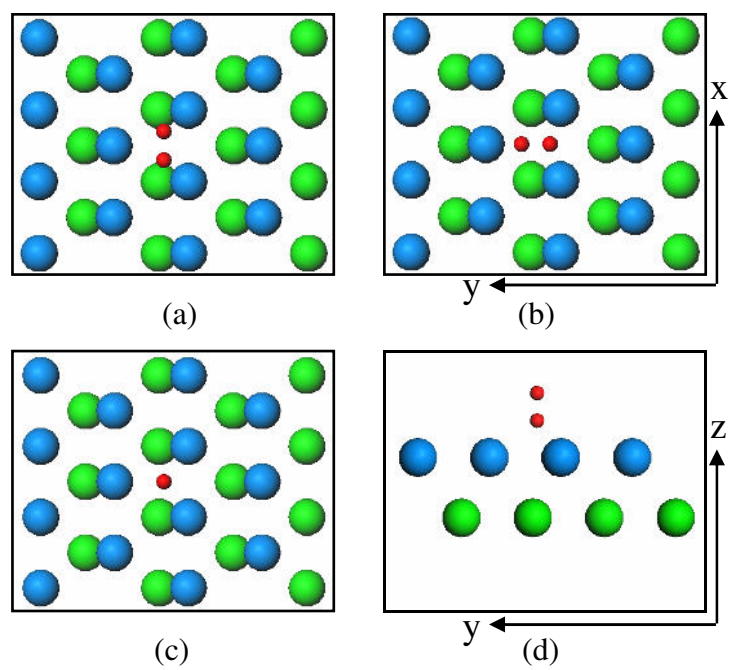
Q.L. Su *et al.* Figure 1

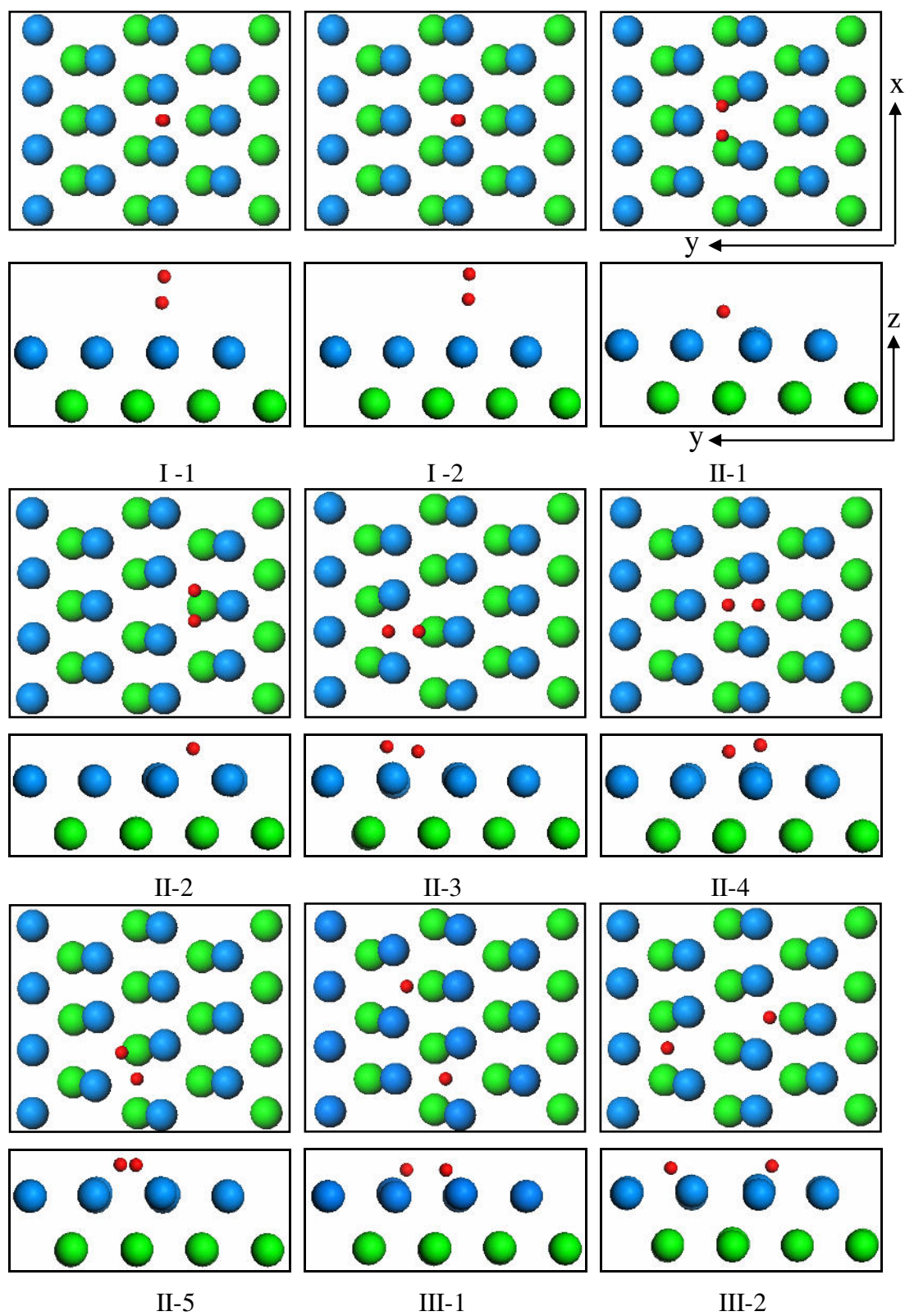
Q.L. Su *et al.* Figure 2

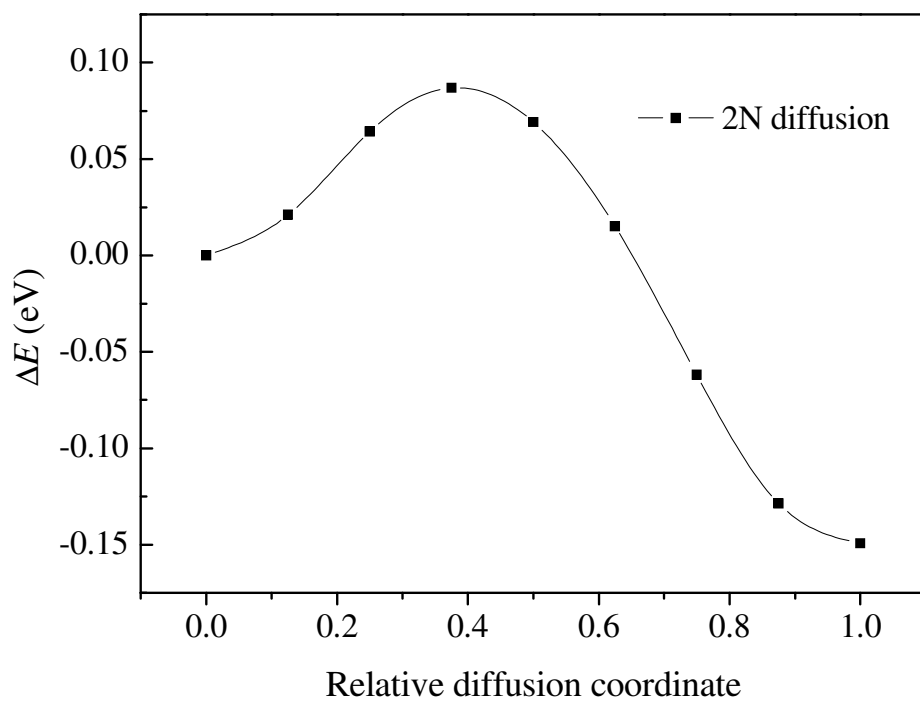
Q.L. Su *et al.* Figure 3

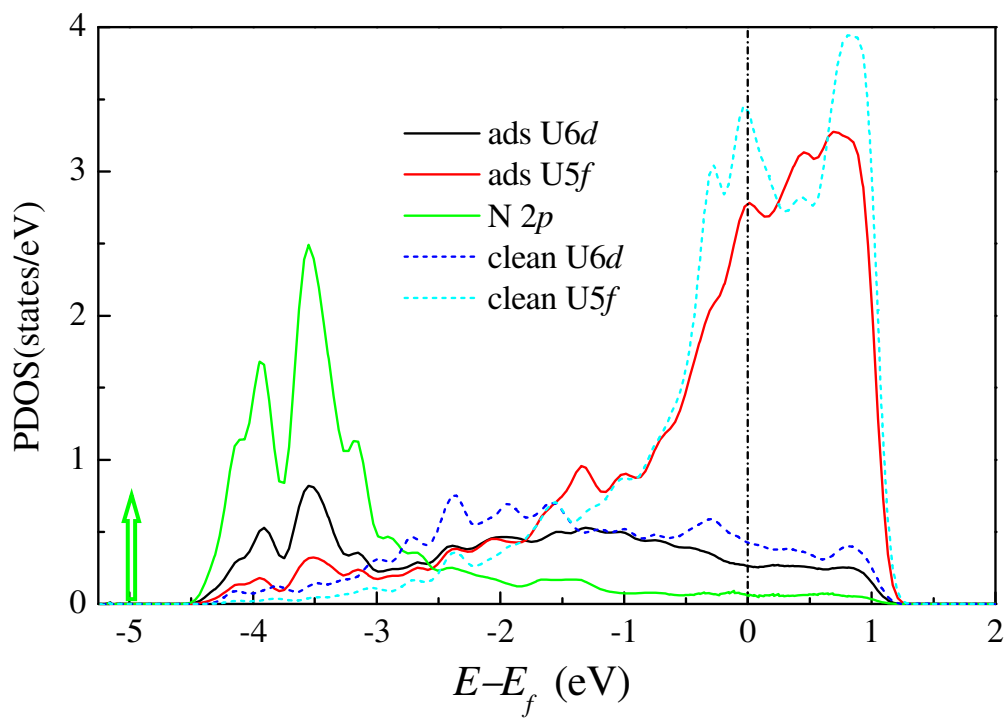
Q.L. Su *et al.* Figure 4

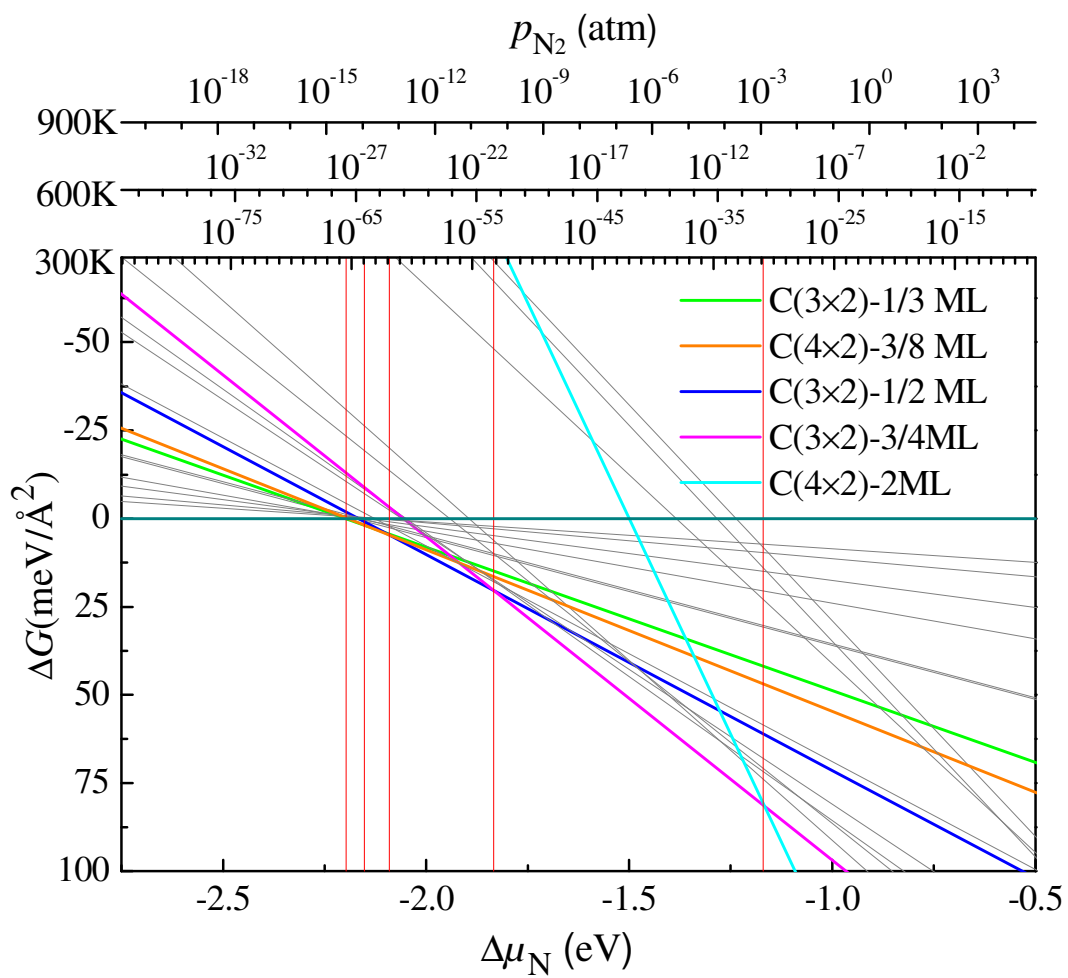
Q.L. Su *et al.* Figure 5

Q.L. Su *et al.* Figure 6

Q.L. Su *et al.* Figure 7

Q.L. Su *et al.* Figure 8

Q.L. Su *et al.* Figure 9

Q.L. Su *et al.* Figure 10